the FEBS Journal

Solution structure of hirsutellin A – new insights into the active site and interacting interfaces of ribotoxins

Aldino Viegas[1], Elias Herrero-Galán[2], Mercedes Oñaderra[2], Anjos L. Macedo[1] and Marta Bruix[3]

1 REQUIMTE-CQFB, Departemento de Quimica, Faculdade de Ciências e Tecnologia, Universidade Nova de Lisboa, Caparica, Portugal
2 Departemento de Bioquímica y Biología Molecular I, Facultad de Química, Universidad Complutense, Madrid, Spain
3 Departemento de Espectroscopía y Estructura Molecular, Instituto de Química Física 'Rocasolano', Consejo Superior de Investigaciones Cientificas, Madrid, Spain

Keywords
cytotoxic protein; NMR; ribonucleases; RNase T1; structure; α-sarcin

Correspondence
M. Bruix, Departamento de Espectroscopía y Estructura Molecular, Instituto de Química Física 'Rocasolano', Serrano 119, 28006 Madrid, Spain
Fax/Tel: +34 91 561 94 00
E-mail: mbruix@iqfr.csic.es

Database
Structural data has been submitted to the Protein Data Bank and BioMagResBank databases under the accession numbers 2kaa and 16018, respectively

(Received 28 November 2008, revised 20 January 2009, accepted 16 February 2009)

doi:10.1111/j.1742-4658.2009.06970.x

Hirsutellin (HtA) is intermediate in size between other ribotoxins and less specific microbial RNases, and thus offers a unique chance to determine the minimal structural requirements for activities unique to ribotoxins. Here, we have determined the structure of HtA by NMR methods. The structure consists of one α-helix, a helical turn and seven β-strands that form an N-terminal hairpin and an anti-parallel β-sheet, with a characteristic α + β fold and a highly positive charged surface. Compared to its larger homolog α-sarcin, the N-terminal hairpin is shorter and less positively charged. The secondary structure elements are connected by large loops with root mean square deviation (rmsd) values > 1 Å, suggesting some degree of intrinsically dynamic behavior. The active site architecture of HtA is unique among ribotoxins. Compared to α-sarcin, HtA has an aspartate group, D40, replacing a tyrosine, and the aromatic ring of F126, located in the leucine 'environment' close to the catalytic H113 in a similar arrangement to that found in RNase T1. This unique active site structure is discussed in terms of its novel electrostatic interactions to understand the efficient cytotoxic activity of HtA. The contributions of the N-terminal hairpin, loop 2 and loop 5 with regard to protein functionality, protein–protein and protein–lipid interactions, are also discussed. The truncation and reduced charge of the N-terminal hairpin in HtA may be compensated for by the extension and new orientation of its loop 5. This novel orientation of loop 5 re-establishes a positive charge on the side of the molecule that has been shown to be important for intermolecular interactions in ribotoxins.

Ribotoxins are a family of toxic extracellular fungal RNases that display specific ribonucleolytic activity against a single phosphodiester bond in the sarcin/ricin loop of the ribosomal RNA [1–4]. This bond (G4325–A4324 in the 28S subunit) is located at an evolutionarily conserved site with important roles in ribosome function, namely elongation factor 1-dependent binding of aminoacyl-tRNA and elongation factor 2-catalyzed GTP hydrolysis and translocation [5]. Cleavage of this phosphodiester bond results in release of a 400 bp fragment, known as the α fragment, and blocks protein synthesis, leading to cell death by apoptosis [6]. Several ribotoxins have been isolated (clavin [7], c-sarcin [8], gigantin [9] and Aspf 1 [10]), with α-sarcin [11–13] (from *Aspergillus giganteus*) and restrictocin [14,15] (from *A. restrictus*) being the best characterized. The sequence identity between α-sarcin and restrictocin is 85%, and they share a basic pI and common tertiary structure [4,13,14]. They fold into an α + β structure with a central five-stranded antiparallel β-sheet and an

Abbreviation
HtA, hirsutellin A.

α-helix. They are highly twisted in the right-handed sense, creating a convex face against which the α-helix is packed. In addition, the N-terminal residues form a β-hairpin that may be considered as two consecutive minor β-hairpins connected by a hinge region. Furthermore, the nature and location of the catalytic residues as well as the enzymatic mechanism (they are cyclizing RNases) are also conserved [16–18]. For these reasons, ribotoxins may be considered to belong to the larger family of fungal/microbial secreted RNases, usually represented by the nontoxic ribonuclease T1 [19]. The main structural differences between ribotoxins and nontoxic RNases are the length and arrangement of the loops and the N-terminal β-hairpin, which are believed to be responsible for ribotoxin cytotoxicity.

Hirsutellin A (HtA) is a 130-residue extracellular protein produced by the invertebrate fungal pathogen *Hirsutella thompsonii*. This protein displays biological properties similar to those of the α-sarcin family [4,20]. Sequence alignment with microbial RNases and ribotoxins revealed a significant similarity even though the sequence identity between HtA and other ribotoxins is marginal, only about 25%. This is lower than the sequence identity observed among all other known ribotoxins, which is always above 60%. It is suggested that the common structural core is conserved in HtA, with the most significant differences being the length of the loops connecting the α-helical and β-sheet regions and the N-terminal hairpin.

A recent study characterized HtA and evaluated its ribotoxin characteristics [4]. It showed conclusively that HtA is a member of the α-sarcin/restrictocin ribotoxin family. Furthermore, far-UV CD analysis confirmed the predominance of β-structure predicted by the sequence similarity between HtA and α-sarcin. The N-terminal β-hairpin characteristic of ribotoxins is shorter in HtA than in α-sarcin, but this structural motif is still present. The active site residues and catalytic mechanism also appear to be conserved. The putative loop 3 in HtA possesses a net positive charge and hydrophilic properties that are thought to be responsible for interacting with the sarcin/ricin loop, providing HtA with specific ribonuclease activity [4,13,15]. With regard to its interaction with lipid vesicles, HtA and α-sarcin show a significant difference: α-sarcin promotes the aggregation of lipid vesicles but HtA does not. Both proteins change the permeability of membranes but HtA is more efficient. These differences are thought to be related to dissimilarities in loop 2 and the N-terminal β-hairpin, which have been proposed to be specifically involved in vesicle aggregation [21].

In order to better understand the structural requirements for the specific activities of these proteins, fungal HtA was obtained and 2D ^{1}H-NMR methodology [22] was used to determine the three-dimensional structure of HtA in aqueous solution. Our results show that the structure is well determined (pairwise rmsd = 0.98 Å for all backbone atoms), and the global fold is similar to that reported for cytotoxins. However, differences can be found in the conformation of loops, the β-hairpin and the relative position of the catalytic residues in the active site. The results obtained will be discussed and compared with those reported for other members of the fungal extracellular RNase family.

Results

Assignment

The ^{1}H assignments for the backbone and side chains are nearly complete. The observed conformational chemical shifts for alpha and amide protons, calculated as $\delta_{HtA}-\delta_{RC}$ (Fig. 1), resemble those reported for α-sarcin [11]; this suggests that the global fold and 3D structure that are characteristic of the ribotoxin family are present in HtA. Analysis of these assignments provides some interesting clues concerning HtA structure. First, several protons show δ values below 0 ppm. One of these shielded nuclei is a gamma proton of P68 with a chemical shift of −0.32 ppm. Tellingly, the gamma protons of the structurally related P98 in α-sarcin also have low δ values (−0.83 and −0.31 ppm). Second, the labile OH protons of S38, Y70, T92, T112 and Y98 exchange slowly enough with the water molecules to be observable in the NMR spectra, and consequently their resonances could be assigned. All these NMR data clearly indicate that HtA has a compact fold with a tightly structured core.

Disulfide bonds and structure determination

The disulfide pairings of HtA were previously predicted from sequence alignment with other members of the ribotoxin family. Here, we have found experimental evidence by searching for H_{β}–H_{β} and H_{α}–H_{β} NOEs between cysteines. At least one intercysteine NOE could be found for C6–C129 and for C57–C108. The long-range NOEs between residues surrounding the cysteines confirm the cysteine pairing defined here. This pattern agrees with the arrangement present in other ribotoxins, and is fully compatible with the distance restraints discussed below.

After seven cycles of NOE assignment and structure calculation by CYANA/CANDID, a set of 20 structures that satisfy the experimental constraints was obtained. The

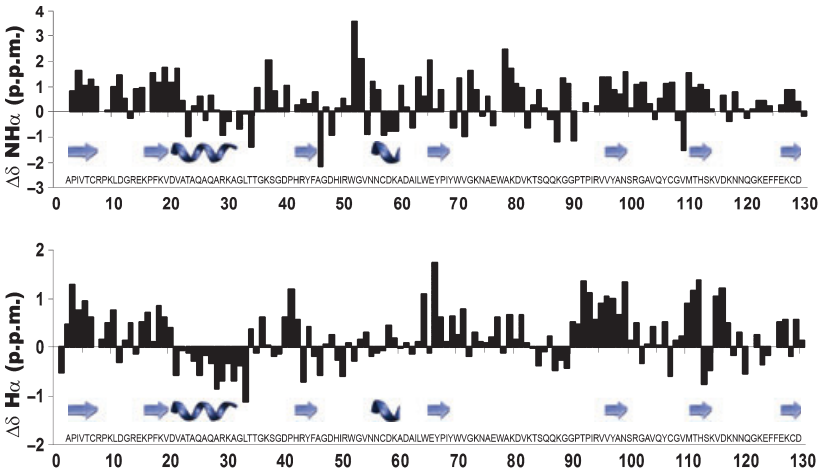

Fig. 1. $^{1}H_{\alpha}$ and $^{1}H_{N}$ conformational shifts ($\delta_{observed}$–$\delta_{random\ coil}$) in ppm for HtA at pH 4.1 and 298 K. The amino acid sequence and the elements of secondary structure are shown; β-strands are represented by arrows and the α-helix by a spiral.

coordinates of these 20 conformers have been deposited in the Research Collaboratory for Structural Bioinformatics Protein Data Bank under accession number 2kaa. The resulting structures satisfied the experimental constraints with small deviations from the idealized covalent geometry, and most of the backbone torsion angles for amino acid residues lie within the allowed regions in the Ramachandran plot. The statistics characterizing the quality and precision of the 20 structures are summarized in Table 1, and a superposition and general view of the structures is shown in Fig. 2A,B. The mean pairwise rmsd value is 0.92 Å for the backbone and 1.62 Å for all heavy atoms. These values decrease to 0.45 and 1.10 Å, respectively, when the regular secondary elements are considered.

Some regions showed mean global displacement values for backbone heavy atoms that were > 1.0 Å, suggesting some degree of intrinsically dynamic behavior. These regions correspond to D11–E14, A46–R51, G53–C57, K83–G89, S101–A104, D117–N119 and G122–F125.

Table 1A. NMR structural calculations summary: restraints used in the structure calculation, and type of distance restraints from NOEs.

Restraints used	
Total distance restraints from NOEs	1988
Total distance restraints from disulfide bonds	12
Total distance restraints from hydrogen bonds	116
Total distance restraints	2104
No. restraints/residue	16.2
Type of restraint	
Short range (li–jl ≤ 1)	939
Medium range (1 < li–jl < 5)	283
Long range (li–jl ≥ 5)	766

Table 1B. Calculation statistics.

	Mean	Minimum	Maximum
CYANA statistics (20 structures)			
Target function (Å^2)	0.78	0.16	1.41
Maximal distance violation (Å)	0.43	0.12	0.62
Average backbone rmsd to mean (cycle 1), residues 1–130	4.70	–	–
Average backbone rmsd to mean (cycle 7), residues 1–130	0.63	–	–
AMBER minimization (20 structures)			
Energy (kcal·mol^{-1})	−2262.34	−3065.02	−1573.28
Maximal distance violation (Å)	0.38	0.17	0.62

Table 1C. Mean pairwise rmsd (Å).

	Backbone	Heavy atoms
Global	0.92 ± 0.13	1.62 ± 0.11
Secondary structure	0.45 ± 0.11	1.10 ± 0.12

Table 1D. PROCHECK analysis.

Ramachandran plot regions	
Favorable	76.8%
Additional	23.0%
Generous	0.2%
Non-favorable	0.0%

Description of hirsutellin A structure

The structure of HtA in solution is similar to those reported for other members of the ribotoxin family (Fig. 2C). It shares the characteristic α + β fold

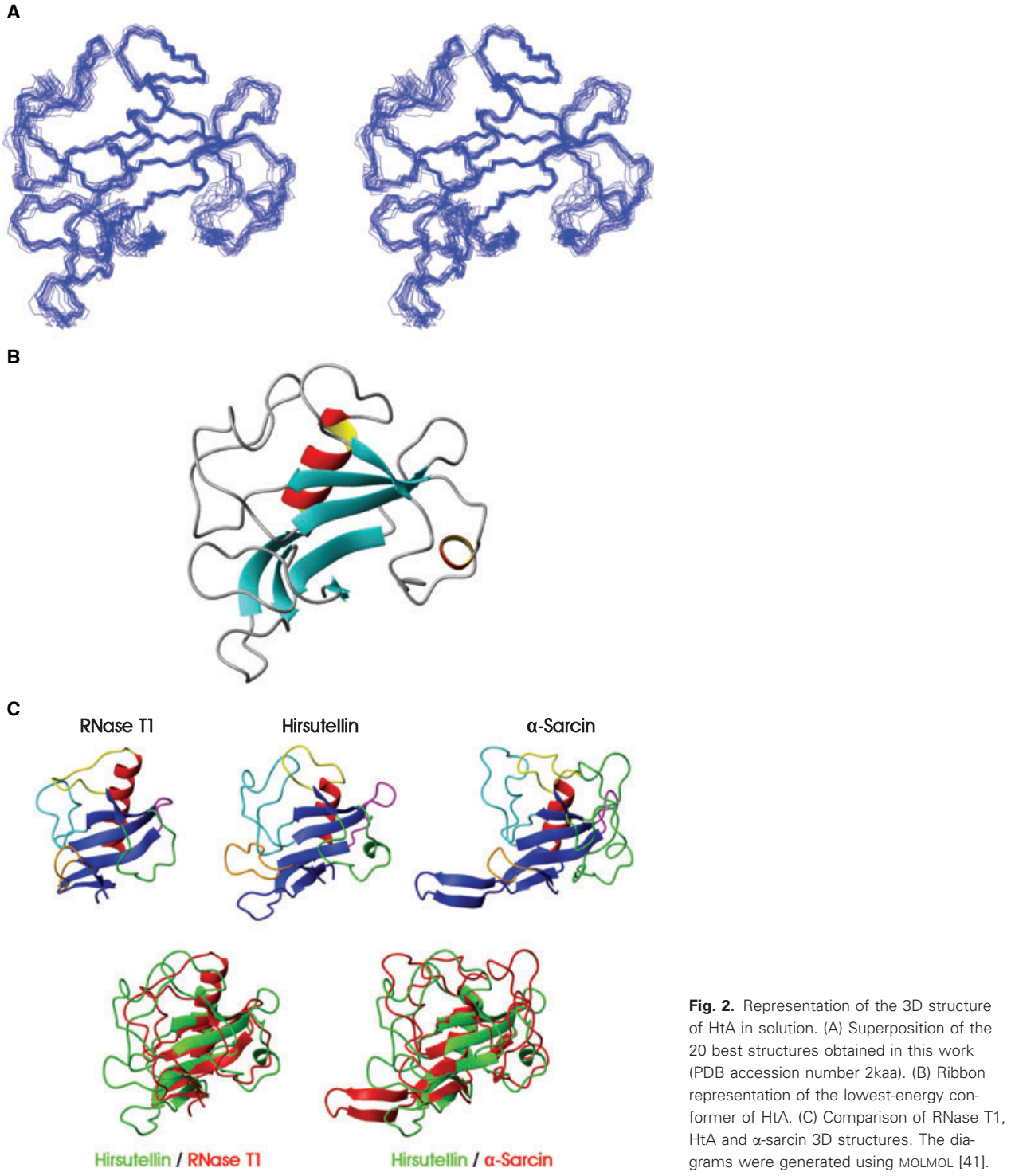

Fig. 2. Representation of the 3D structure of HtA in solution. (A) Superposition of the 20 best structures obtained in this work (PDB accession number 2kaa). (B) Ribbon representation of the lowest-energy conformer of HtA. (C) Comparison of RNase T1, HtA and α-sarcin 3D structures. The diagrams were generated using MOLMOL [41].

stabilized by two disulfide bridges (C6–C129, C57–C108) with a highly positive charged surface. The structure contains an α-helix (α_1, V21–A31), a single helix turn (α_2, N56–D58) and seven β-strands (β_1, I3–C6; β_2, F17–D20; β_3, H42–Y44; β_4, L64–P68; β_5, R95–A99; β_6, G109–H113; β_7: F126–K128). The β-strands form an N-terminal hairpin (β_1 and β_2) and an antiparallel β-sheet (β_3–β_7). The remaining residues of the HtA sequence form large loops connecting the secondary structure elements. As in other ribotoxins, these

loops are well defined despite their lack of regular secondary structures. For instance, loop 2 is shorter in HtA than in α-sarcin, but the structure of the remaining part is the same in both proteins, including a short segment (N56, C57 and D58) forming a turn of 3_{10} helix (D75, C76 and D77 in α-sarcin).

The active site

The active site is composed of well-defined side chains mainly corresponding to the charged amino acids D40, H42, E66, R95 and H113, together with the aromatic ring of F126 (Fig. 3A). Three interesting differences were observed compared with the active site of the ribotoxins α-sarcin and restrictocin (Fig. 3B). On the basis of its sequence alignment, which matched it with Y48 in α-sarcin, Y44 was proposed to be part of the active site. However, in the 3D structure, the orientation of this group is completely different from that of Y48 in α-sarcin. This suggests that Y44 in HtA does not form part of the active site, and, consequently, does not perform the same role as Y48 does in α-sarcin, namely stabilizing the intermediate in the transphosphorylation reaction [14]. The second novelty is the presence of a carboxylate group belonging to D40. This side chain is very well positioned to interact electrostatically with the other charged groups. In the NMR structures, this side chain of D40 is a short distance (≤ 3 Å) from the side chains of H42 and R95. Finally, the aromatic ring of F126, placed close to the catalytic H113, is in a similar orientation to that in the active site of nonspecific RNases. These novel architectural features lead to new electrostatic interactions at the active site of this ribotoxin. They are important for protein activity as electrostatic interactions define the characteristic microenvironment in α-sarcin [23,24] that is responsible for its efficient cytotoxic action.

Discussion

As is very well documented, ribotoxins and nonspecific ribonucleases show high structural homology but different specific activities. Although classic ribotoxins such as α-sarcin and restrictocin (about 150 amino acids) are larger than nontoxic RNases (about 96–110 amino acids), they share a similar central structured region connected by loops of different length. Indeed, extended loops and the N-terminal β-hairpin have been proposed to be the structural determinants responsible for ribotoxin properties [13].

HtA has emerged as a novelty in this field. It has been demonstrated that it is a ribotoxin but it has an intermediate size between classical ribotoxins and nonspecific RNases [4] (Fig. 2). *A priori*, HtA could be considered as an evolutionary intermediate that may share properties of both protein families, or at least have acquired some of the properties of the highly evolved cytotoxins. However, this does not appear to be the case, as HtA has all the specific properties of a cytotoxin despite its short sequence (130 amino acids). This suggests that HtA is not an evolutionary intermediate, but has actually evolved further than other ribotoxins to become smaller and more economical.

At the same time, the active site of HtA, as revealed by the 3D structure, shows a different arrangement to that shown by the classical ribotoxins, but catalyzes the same hydrolytic reaction with similar efficiency. Hence description of the new interactions established in the active site is also of relevance.

The active site: structural and electrostatic basis of HtA function

The reaction catalyzed by ribotoxins follows a mechanism of transphosphorylation, which implies the

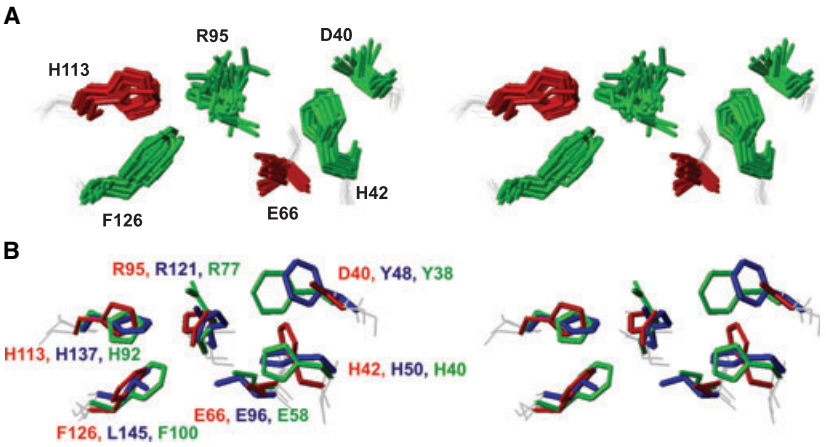

Fig. 3. Stereo diagram of the active center of HtA. (A) Superposition of the active-site residues of the 20 conformers of the solution structure of HtA. Catalytic groups E66 and H113 are shown in red, and side chains of other residues in their vicinity are shown in green. (B) Superposition of the active-site residues of HtA (red), α-sarcin (blue) and RNase T1 (green).

involvement of a catalytic pair constituted by an acid and a base on each side of the hydrolyzed bond [16]. E96 and H137 in α-sarcin and E58 and H92 in RNase T1 act as the base and acid groups, respectively. Comparing the 3D structures, E66 and H113 in HtA are in similar positions to those pairs and may be considered to be the catalytic residues. A superposition of the active site of RNase T1, α-sarcin and HtA is shown in Fig. 3B. It is known that other side chains in the vicinity of these amino acids are also important for the activity. Given the 3D structure of the HtA active site, and the interactions between side chains, we propose that D40, H42, R95 and F126 also form part of it. As in other ribotoxins, the active site of HtA is buried, with the accessible surface area of the corresponding side chains very low. Desolvation of the charged groups should affect their pK_a values, increasing the pK_a of carboxylates and decreasing the pK_a of histidines [24].

Structurally, the architecture of the active site in HtA is unique among the ribotoxin members. It has an aromatic ring (like nontoxic RNases but unlike ribotoxins), which is in a position to be able to interact with the catalytic histidine [25]. This interaction between the side chains of H113 and F126 could electrostatically stabilize the positive imidazole charge in this low di-electric environment, increasing its pK_a value. It is known that the presence of a cation–π interaction is crucial in determining the pK_a of the histidine residue in the active site of RNases and consequently in determining the activity profile of this enzyme as a function of pH [26,27]. Another unique feature of the HtA active centre is that H42 (corresponding to H50 in α-sarcin) shows an alternative conformation in which it is pointing towards the negatively charged D40. This position should favor a salt bridge interaction that will decrease the pK_a of the aspartic acid and increase the pK_a of the histidine side chain groups. Finally, E66 and R95 are in their canonical positions but establish different interactions to those in other ribotoxin active sites. It is well known that the catalytic process in ribotoxins is extremely dependent on the microstructural and electrostatic environment of the active site. The specific properties described above could explain why the optimum pH for degradation of dinucleotide phosphates is in the range 7–8, and the peculiar activity profile as a function of pH [4]. The pH of maximum activity *in vitro* resembles that shown by RNase T1 [19], and the profile is complex, showing a main curve with a shoulder at acidic pH, suggesting the presence of two different mechanisms as observed in α-sarcin [23]. These facts are in concordance with the complexity of the active site of HtA, involving the new electrostatic interactions described here for ribotoxins for the first time. However, more work is necessary to study the role of the various groups in determining the dependence of the activity on pH.

Comparison with other structures: structural properties of HtA regions involved in protein–protein or protein–lipid interactions

The core structure adopted by HtA in solution is similar to those of ribotoxins and microbial RNases. They share the same central β-sheet, and, as in α-sarcin, the helix of HtA (residues 21–31) is shorter than that of RNase T1 (residues 13–29). These regions are connected by long loops that are slightly shorter (loop 1, residues 32–41), slightly longer (loops 3 and 5, residues 68–94 and 114–125), and of similar length (loop 4, residues 99–108) when compared with classical ribotoxins. With regard to function, the most relevant differences are the shorter length of loop 2 and the N-terminal β-hairpin, as discussed below.

Like α-sarcin, HtA specifically degraded ribosomes producing the α fragment [1,28]. Recently, the importance of the N-terminal hairpin and loop 2 of ribotoxins in protein functionality and protein–protein and protein–lipid interactions has been demonstrated [10,29–31]. Thus, the first segment of the long loop 2 in α-sarcin has been proposed to be involved in substrate recognition [15]. The conformation of this region is stabilized in part by a specific hydrogen bond between N54 and I69. This interaction is conserved in all microbial RNases and contributes significantly to the overall stability [32]. In HtA, the equivalent positions, D48 and I50 respectively, lie near to each other due to loop 2 being shorter. This indicates that, in order to maintain the specific conformation of the common part of loop 2, the hydrogen bond in α-sarcin links two segments that are already close in HtA.

On the basis of a docking model [33], it was proposed that α-sarcin interacts with protein L14 in the ribosome through the basic region of the N-terminal hairpin involving residues K11, K14, K17 and K21, and with ribosomal protein L6 through the highly basic part of loop 2 containing residues K61, K64, K70, K73, K81, K84 and K89. These two regions have also been proposed to be involved in membrane interaction. The length of the N-terminal hairpin in HtA is intermediate between those in RNse T1 and α-sarcin, having 20 amino acids in HtA, 26 in α-sarcin and 12 in RNase T1. From a functional point of view, this reduction in length and charge (two positive residues are missing) with respect to ribotoxins could be related

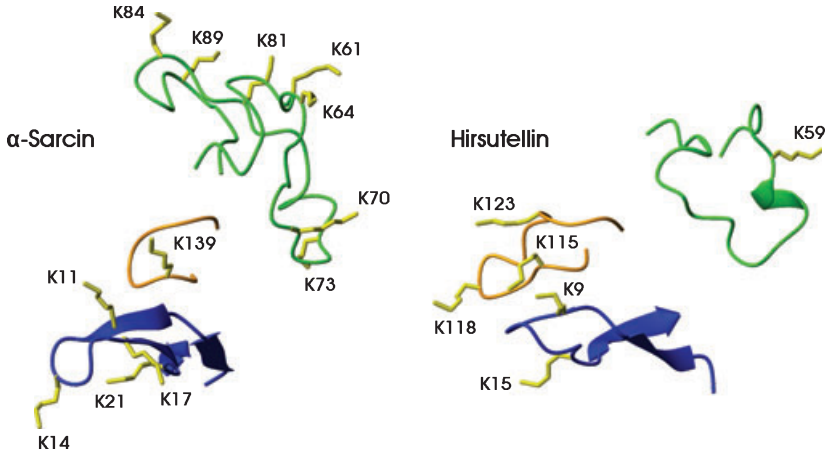

Fig. 4. Comparison of the spatial orientation of the N-terminal β-hairpin and loops 2 and 5 in HtA and α-sarcin. The backbone trace is represented in blue for the β-hairpin, orange for loop 5, and green for loop 2. Side chains of lysine residues are shown in yellow.

to the extension of loop 5 of HtA (Fig. 4). In fact, loop 5 in HtA adopts a new orientation pointing towards the closed end of the short hairpin. This allows the extra region of loop 5, which includes three lysine residues K115, K118 and K123, to compensate for the lack of charge on that face of the molecule. These positive charges have been shown to be important for intermolecular interactions of α-sarcin with the ribosome and vesicles. In this sense, loop 2 could also be related to membrane interaction.

These proteins also interact with acid phospholipids in the first step of the cytotoxic action. However, the interaction is different in HtA and sarcin. Whereas α-sarcin promotes vesicle aggregation and leakage of vesicle contents, HtA does not promote lipid oligomerization. The highly charged loop 2 and N-terminal hairpin in sarcin were proposed to be the regions involved in lipid interactions [21]. In HtA, loop 2 (residues 45–63) is much shorter than in α-sarcin (19 amino acids versus 41 amino acids, respectively), and lacks the above-mentioned positively charged region that is able to interact with phospholipid vesicles (Fig. 4).

Conclusion

In summary, this work focused on understanding the structural requirements for the general ribonucleolytic and cytotoxic activities of the protein HtA. With this aim, we determined the structure of HtA by ^{1}H-NMR methods, and the possible structure–function relationships have been discussed. The solution structure is similar to those reported for other members of the ribotoxins family, with a characteristic α + β fold and a highly positive charged surface. Interestingly, the architecture of the active site of HtA was found to be unique among the ribotoxin family members. D40 in HtA replaces a tyrosine of α-sarcin, and the aromatic ring of F126, close to the catalytic H113, replaces a leucine side chain in α-sarcin in a similar arrangement to that found in RNase T1. This unique active site structure establishes new electrostatic interactions, described for the first time in ribotoxins, that determine cytotoxic efficiency in HtA. It is remarkable that the exquisite specificity of the ribotoxins HtA and α-sarcin can be achieved by two quite different sets of active site residues.

Experimental procedures

Protein isolation and purification

Fungal wild-type HtA was obtained from broth cultures of *Hirsutella thompsonii* var. *thompsonii* HTF72 as described previously [4]. Modifications to previous purification methods [34,35] were introduced in order to achieve a higher purity with better yields. Culture filtrates were run through two ion-exchange columns, first on DEAE-cellulose (DE52 Whatman) equilibrated in 50 mM Tris, pH 8.0, and then on CM-cellulose (CM52 Whatman) equilibrated in 50 mM sodium acetate, pH 5.0, containing 0.1 M NaCl. The protein was eluted from the second column using a 600 mL linear gradient (0.25–0.4 M NaCl in the same buffer) to achieve complete separation from a major contaminant. The samples were analyzed by polyacrylamide gel electrophoresis, protein hydrolysis and amino acid analysis, and Western blots were done using a mouse monoclonal antiserum raised against natural HtA.

NMR spectroscopy and assignment

HtA samples were prepared for NMR experiments at 0.7 mM in 90% H_2O/10%D_2O or in D_2O containing sodium-4,4-dimethyl-4-silapentane-1-sulfonate (DSS) at pH 4.1 and 5.5. NMR spectra were obtained at 308 or 298 K on a Bruker AV 800 NMR spectrometer (Bruker,

Karlsruhe, Germany) equipped with a triple-resonance cryoprobe and an active shielded *z*-gradient coil, or with a conventional TXI probe and *x*-, *y*- and *z*-gradients. Traditional 2D COSY, TOCSY (60 ms mixing time) and NOESY (50 and 80 ms mixing times) spectra were acquired in H_2O and D_2O. Processing of the spectra was performed using the program TOPSPIN (Bruker). Analysis of the spectra, manual assignment of backbone and side-chain protons, and cross-peak area calculations were performed using Sparky [36].

Assignments were performed using classical NOE-based methodology [22]. The final assignments of the ^1H resonances have been deposited in the BioMagResBank database [37] under accession number 16018.

Structure calculation

After assignment completion, peak data from NOESY spectra were analyzed in a semi-automated iterative manner by CYANA 2.1 [38]. The NOE coordinates and intensities used as input for automated analysis were generated automatically by Sparky based on the chemical shift list generated in the assignment process. The unambiguous NOEs assigned to a given pair of protons were converted into upper limits by CYANA. Additionally, standard upper and lower limits for each of the two disulfide bonds (6–129, 57–108) were introduced during the rounds of calculations [2.1/2.0 Å for Sγ(i)–Sγ(j) and 3.1/3.0 for Cβ(i)–Sγ(j) and Sγ(i)–Cβ(j)]. No stereospecific assignments were introduced initially. In the final steps, 50 pairs of stereospecific limits were introduced by CYANA for the structure calculations.

Hydrogen bond constraints were applied at a late stage of the structure calculation if characteristic NOE patterns were observed for α-helices or β-strands and slowly exchanging amide groups were identified in D_2O. This information was used by CYANA/CANDID to compute seven cycles of NOE cross-peak assignment and structure calculation, each with 100 starting structures. After the first few rounds of calculations, the spectra were analyzed again to identify additional cross-peaks consistent with the structural model and to remove mis-identified peaks. Input data and structure calculation statistics are summarized in Table 1. The 20 structures with the lowest final CYANA target function values were then subjected to restrained energy minimization using the AMBER force field [39], and used to characterize the solution structure of the HtA protein. PROCHECK-NMR version 3.4.4 [40] was used to analyze the quality of the refined structures, and MOLMOL [41] was used to visualize them, calculate accessibilities, and to prepare the diagrams of the molecules.

Acknowledgements

This paper was supported by projects GRICES-CSIC 2007-2008, BFU2005-01855/BMC and BFU2006-04404 of the Spanish Ministerio de Educación y Ciencia, and SFRH/BD/35992/2007 of the Portuguese Science and Technology Foundation.

References

1 Schindler DG & Davies JE (1977) Specific cleavage of ribosomal RNA caused by alpha sarcin. *Nucleic Acids Res* **4**, 1097–1110.
2 Martínez-Ruiz A, García-Ortega L, Kao R, Lacadena J, Oñaderra M, Mancheño JM, Davies J, Martínez del Pozo A & Gavilanes JG (2001) RNase U2 and alpha-sarcin: a study of relationships. *Meth Enzymol* **341**, 335–351.
3 Lacadena J, Álvarez-García E, Carreras-Sangra N, Herrero-Galán E, Alegre-Cebollada J, García-Ortega L, Oñaderra M, Gavilanes JG & Martínez del Pozo A (2007) Fungal ribotoxins: molecular dissection of a family of natural killers. *FEMS Microbiol Rev* **31**, 212–237.
4 Herrero-Galán E, Lacadena J, Martínez Del Pozo A, Boucias DG, Olmo N, Oñaderra M & Gavilanes JG (2008) The insecticidal protein hirsutellin A from the mite fungal pathogen *Hirsutella thompsonii* is a ribotoxin. *Proteins* **72**, 217–228.
5 Wool IG, Gluck A & Endo Y (1992) Ribotoxin recognition of ribosomal RNA and a proposal for the mechanism of translocation. *Trends Biochem Sci* **17**, 266–269.
6 Olmo N, Turnay J, González de Buitrago G, López de Silanes I, Gavilanes JG & Lizarbe MA (2001) Cytotoxic mechanism of the ribotoxin α-sarcin. Induction of cell death via apoptosis. *Eur J Biochem* **268**, 2113–2123.
7 Parente D, Raucci G, Celano B, Pacilli A, Zanoni L, Canevari S, Adobati E, Colnaghi MI, Dosio F, Arpicco S *et al.* (1996) Clavin, a type-1 ribosome-inactivating protein from *Aspergillus clavatus* IFO 8605. cDNA isolation, heterologous expression, biochemical and biological characterization of the recombinant protein. *Eur J Biochem* **239**, 272–280.
8 Huang KC, Hwang YY, Hwu L & Lin A (1997) Characterization of a new ribotoxin gene (c-*sar*) from *Aspergillus clavatus*. *Toxicon* **35**, 383–392.
9 Wirth J, Martinez del Pozo A, Mancheno JM, Martinez-Ruiz A, Lacadena J, Onaderra M & Gavilanes JG (1997) Sequence determination and molecular characterization of gigantin, a cytotoxic protein produced by the mould *Aspergillus giganteus* IFO 5818. *Arch Biochem Biophys* **343**, 188–193.
10 García-Ortega L, Lacadena J, Villalba M, Rodríguez R, Crespo JF, Rodríguez J, Pascual C, Olmo N, Oñaderra M, del Pozo AM *et al.* (2005) Production and characterization of a noncytotoxic deletion variant of the *Aspergillus fumigatus* allergen Aspf1 displaying reduced IgE binding. *FEBS J* **272**, 2536–2544.

11 Campos-Olivas R, Bruix M, Santoro J, Martínez del Pozo A, Lacadena J, Gavilanes JG & Rico M (1996) ^{1}H and ^{15}N nuclear magnetic resonance assignment and secondary structure of the cytotoxic ribonuclease α-sarcin. *Protein Sci* **5**, 969–972.
12 Campos-Olivas R, Bruix M, Santoro J, Martínez del Pozo A, Lacadena J, Gavilanes JG & Rico M (1996) Structural basis for the catalytic mechanism and substrate specificity of the ribonuclease alpha-sarcin. *FEBS Lett* **399**, 163–165.
13 Pérez-Cañadillas JM, Santoro J, Campos-Olivas R, Lacadena J, Martínez del Pozo A, Gavilanes JG, Rico M & Bruix M (2000) The highly refined solution structure of the cytotoxic ribonuclease α-sarcin reveals the structural requirements for substrate recognition and ribonucleolytic activity. *J Mol Biol* **299**, 1061–1073.
14 Yang X & Moffat K (1996) Insights into specificity of cleavage and mechanism of cell entry from the crystal structure of the highly specific *Aspergillus* ribotoxin, restrictocin. *Structure* **4**, 837–852.
15 Yang X, Gérczei T, Glover LT & Correll CC (2001) Crystal structures of restrictocin–inhibitor complexes with implications for RNA recognition and base flipping. *Nat Struct Biol* **8**, 968–973.
16 Lacadena J, Martínez del Pozo A, Lacadena V, Martínez-Ruiz A, Mancheño JM, Oñaderra M & Gavilanes JG (1998) The cytotoxin α-sarcin behaves as a cyclizing ribonuclease. *FEBS Lett* **424**, 46–48.
17 Lacadena J, Martínez del Pozo A, Martínez-Ruiz A, Pérez-Cañadillas JM, Bruix M, Mancheño JM, Oñaderra M & Gavilanes JG (1999) Role of histidine-50, glutamic acid-96, and histidine-137 in the ribonucleolytic mechanism of the ribotoxin α-sarcin. *Proteins* **37**, 474–484.
18 Álvarez-García E, García-Ortega L, Verdún Y, Bruix M, Martínez del Pozo A & Gavilanes JG (2006) Tyr-48, a conserved residue in ribotoxins, is involved in the RNA-degrading activity of α-sarcin. *Biol Chem* **387**, 535–541.
19 Steyaert J (1997) A decade of protein engineering on ribonuclease T1 – atomic dissection of the enzyme–substrate interactions. *Eur J Biochem* **247**, 1–11.
20 Martínez-Ruiz A, Martínez del Pozo A, Lacadena J, Oñaderra M & Gavilanes JG (1999) Hirsutellin A displays significant homology to microbial extracellular ribonucleases. *J Invertebr Pathol* **74**, 96–97.
21 Mancheño JM, Gasset M, Lacadena J, Ramon F, Martínez del Pozo A, Oñaderra M & Gavilanes JG (1994) Kinetic study of the aggregation and lipid mixing produced by α-sarcin on phosphatidylglycerol and phosphatidylserine vesicles: stopped-flow light scattering and fluorescence energy transfer measurements. *Biophys J* **67**, 1117–1125.
22 Wüthrich K (1986) *NMR of Proteins and Nucleic Acids*. Wiley, New York, NY.
23 Pérez-Cañadillas JM, Campos-Olivas R, Lacadena J, Martínez del Pozo A, Gavilanes JG, Santoro J, Rico M & Bruix M (1998) Characterization of pKa values and titration shifts in the cytotoxic ribonuclease α-sarcin by NMR. Relationship between electrostatic interactions, structure, and catalytic function. *Biochemistry* **37**, 15865–15876.
24 García-Mayoral MF, Pérez-Cañadillas JM, Santoro J, Ibarra-Molero B, Sánchez-Ruiz JM, Lacadena J, Martínez del Pozo A, Gavilanes JG, Rico M & Bruix M (2003) Dissecting structural and electrostatic interactions of charged groups in α-sarcin. An NMR study of some mutants involving the catalytic residues. *Biochemistry* **42**, 13122–13133.
25 Doumen J, Gonciarz M, Zegers I, Loris R, Wyns L & Steyaert J (1996) A catalytic function for the structurally conserved residue Phe 100 of ribonuclease T1. *Protein Sci* **5**, 1523–1530.
26 Masip M, García-Ortega L, Olmo N, García-Mayoral MF, Pérez-Cañadillas JM, Bruix M, Oñaderra M, Martínez del Pozo A & Gavilanes JG (2003) Leucine 145 of the ribotoxin α-sarcin plays a key role for determining the specificity of the ribosome-inactivating activity of the protein. *Protein Sci* **12**, 161–169.
27 García-Mayoral MF, del Pozo AM, Campos-Olivas R, Gavilanes JG, Santoro J, Rico M, Laurents DV & Bruix M (2006) pH-dependent conformational stability of the ribotoxin α-sarcin and four active site charge substitution variants. *Biochemistry* **45**, 13705–13718.
28 Endo Y & Wool IG (1982) The site of action of alpha-sarcin on eukaryotic ribosomes. The sequence at the α-sarcin cleavage site in 28S ribosomal ribonucleic acid. *J Biol Chem* **257**, 9054–9060.
29 García-Ortega L, Lacadena J, Mancheño JM, Oñaderra M, Kao R, Davies J, Olmo N, Pozo AM & Gavilanes JG (2001) Involvement of the amino-terminal β-hairpin of the *Aspergillus* ribotoxins on the interaction with membranes and nonspecific ribonuclease activity. *Protein Sci* **10**, 1658–1668.
30 García-Ortega L, Masip M, Mancheño JM, Oñaderra M, Lizarbe MA, García-Mayoral MF, Bruix M, Martínez del Pozo A & Gavilanes JG (2002) Deletion of the NH_2-terminal β-hairpin of the ribotoxin α-sarcin produces a nontoxic but active ribonuclease. *J Biol Chem* **277**, 18632–18639.
31 García-Mayoral MF, García-Ortega L, Lillo MP, Santoro J, Martínez del Pozo A, Gavilanes JG, Rico M & Bruix M (2004) NMR structure of the noncytotoxic α-sarcin mutant Δ(7-22): the importance of the native conformation of peripheral loops for activity. *Protein Sci* **13**, 1000–1011.
32 Hebert EJ, Giletto A, Sevcik J, Urbanikova L, Wilson KS, Dauter Z & Pace CN (1998) Contribution of a conserved asparagine to the conformational stability of

ribonucleases Sa, Ba, and T1. *Biochemistry* **37**, 16192–16200.
33 García Mayoral F, García-Ortega L, Álvarez-García E, Bruix M, Gavilanes JG & del Pozo AM (2005) Modeling the highly specific ribotoxin recognition of ribosomes. *FEBS Lett* **579**, 6859–6864.
34 Mazet I & Vey A (1995) Hirsutellin A, a toxic protein produced in vitro by *Hirsutella thompsonii*. *Microbiology* **141**, 1343–1348.
35 Liu WZ, Boucias DG & McCoy CW (1995) Extraction and characterization of the insecticidal toxin hirsutellin A produced by *Hirsutella thompsonii* var. *thompsonii*. *Exp Mycol* **19**, 254–262.
36 Goddard TD & Kneller DG. *SPARKY 3*. University of California, San Francisco, CA. http://www.cgl.ucsf.edu/home/sparky/.
37 Ulrich EL, Akutsu H, Doreleijers JF, Harano Y, Ioannidis YE, Lin J, Livny M, Mading S, Maziuk D, Miller Z *et al*. (2008) BioMagResBank. *Nucleic Acids Res* **36**, D402–D408.
38 Güntert P (2004) Automated NMR structure calculation with CYANA. *Methods Mol Biol* **278**, 353–378.
39 Weiner SJ, Kollman PA, Case DA, Singh UC, Ghio C, Alagona G, Profeta S & Weiner P (1984) A new force field for molecular mechanical simulation of nucleic acids and proteins. *J Am Chem Soc* **106**, 765–784.
40 Laskowski RA, Rullmannn JA, MacArthur MW, Kaptein R & Thornton JM (1996) AQUA and PROCHECK-NMR: programs for checking the quality of protein structures solved by NMR. *J Biomol NMR* **8**, 477–486.
41 Koradi R, Billeter M & Wüthrich K (1996) MOLMOL: a program for display and analysis of macromolecular structures. *J Mol Graph* **14**, 51–55.